

# MiR-129-2 weakens proliferation and promotes apoptosis of liver cancer cells by suppressing the Wnt signaling pathway

Q.-C. MAI<sup>1,2</sup>, Z.-O. MO<sup>1</sup>, J. HE<sup>1</sup>, Q. GOU<sup>1</sup>, F. SHI<sup>1</sup>, W.-H. ZHUANG<sup>1</sup>, R.-D. XU<sup>1</sup>, W.-K. LI<sup>1</sup>, Z.-J. ZHOU<sup>1</sup>, X.-M. CHEN<sup>1,2</sup>

<sup>1</sup>Department of Interventional Oncology, Guangdong Provincial People's Hospital, Guangdong Academy of Medical Sciences, Guangzhou, China

<sup>2</sup>The Second School of Clinical Medicine, Southern Medical University, Guangzhou, China

*Qicong Mai and Zhiqiang Mo contributed equally to this work*

**Abstract. – OBJECTIVE:** To explore the effects of micro ribonucleic acid-129-2 (miR-129-2) on proliferation and migration of liver cancer cells and its possible mechanism.

**PATIENTS AND METHODS:** The expression level of miR-129-2 was measured in liver cancer tissues and adjacent tissues from patients with liver cancer. Its level in liver cancer HepG2 cells and normal liver cells L-02 was also detected via quantitative polymerase chain reaction (qPCR). MiR-129-2 overexpression model was established in the HepG2 cell line. The proliferation and apoptosis levels of cells were determined by methyl thiazolyl tetrazolium (MTT) assay and flow cytometry, respectively. Wound healing assay was performed to detect the migration ability of cells. The expressions level of genes in the Wnt signaling pathway were measured through Western blotting. Xenograft tumor model was conducted in nude mice for exploring the *in vivo* effects of miR-129-2 on liver cancer growth.

**RESULTS:** The expression level of miR-129-2 was significantly lower in liver cancer tissues than that in adjacent tissues ( $p < 0.01$ ), and it was overtly lower in HepG2 cells than that in L-02 cells ( $p < 0.01$ ). Overexpression of miR-129-2 weakened proliferation and migration abilities of liver cancer cells ( $p < 0.01$ ), and evidently increased apoptosis level ( $p < 0.01$ ). Sex-determining region Y-related HMG-box 4 (Sox4) and matrix metalloproteinase-2 (MMP-2) were downregulated, while phosphorylated glycogen synthase kinase-3 $\beta$  (p-GSK3 $\beta$ ) was upregulated in liver cancer cells overexpressing miR-129-2. Besides, the weight and volume of tumors in nude mice bearing liver cancer were significantly smaller after overexpression of miR-129-2.

**CONCLUSIONS:** MiR-129-2 weakens proliferation and migration and stimulates apoptosis in liver cancer cells mainly by downregulating Sox4 and inactivating the Wnt signaling pathway.

**Key Words:**

MiR-129-2, Liver cancer, Proliferation, Migration.

## Introduction

Liver cancer, one of the most common malignancies in clinical practice, is characterized by high malignancy, high mortality rate, and poor prognosis. The annual deaths from liver cancer in China account for more than half of the total cases<sup>1,2</sup>. Surgical resection is the first choice for patients with liver cancer. However, some patients do not meet the indications for surgical resection because they are already in the middle or advanced stage when diagnosed<sup>3</sup>. In addition, liver transplantation, chemotherapy, and interventional therapy are also commonly applied, which markedly prolong the 5-year survival rate of patients with liver cancer<sup>4</sup>. High postoperative recurrence rate, severe side effects of chemotherapy, and lack of liver donor resources result in high mortality and poor prognosis in liver cancer<sup>5</sup>. As molecular biology and genomics rapidly develop, growing evidence<sup>6</sup> has demonstrated that micro ribonucleic acids (miRNAs) have close correlations with the development and progression of tumors. MiRNAs are a kind of endogenous, non-coding, single-stranded small RNAs in eukaryotic cells. MiR-129-2, a member of miRNAs, is located on chromosome 11p11.2 and it participates in regulating the development of gastric cancer, bladder cancer, and other malignant tumors<sup>7</sup>. Klangjorhor et al<sup>8</sup> revealed that overexpressing miR-129-2 down-regulates the expression of sex-determining region Y-related HMG-box 4 (Sox4) in os-

teosarcoma cells and inhibits the Wnt signaling pathway, thereby repressing proliferation and migration of osteosarcoma cells. The correlations between the proliferation and migration of liver cancer cells with miR-129-2 have not yet been explored so far. This paper, therefore, aims to investigate the biological functions of miR-129-2 in liver cancer, so as to provide a theoretical basis for the further exploration of pathogenesis of liver cancer and the search for new therapeutic targets.

## Patients and Methods

### Sample Collection

A total of 20 cases of liver cancer tissues and adjacent tissues from liver cancer patients treated in our hospital from 2015 to 2018 were collected. All samples were definitely diagnosed as liver cancer tissues or adjacent tissues *via* pathological examination. This investigation was approved by the Ethics Committee of Guangdong Provincial People's Hospital. Signed written informed consents were obtained from all participants before the study.

### Cell Culture

Liver cancer cell line HepG2 and normal liver cell line L-02 were purchased from American Type Culture Collection (ATCC; Manassas, VA, USA). They were cultured in Dulbecco's Modified Eagle's Medium (DMEM; Gibco, Rockville, MD, USA) containing 10% fetal bovine serum (FBS; Gibco, Rockville, MD, USA) in a 5% CO<sub>2</sub> incubator at 37°C. Thereafter, the cells that grew to the logarithmic growth phase at a density of about 80% were passaged until the third generation. Next, the cells were inoculated in a 6-well plate at 10<sup>5</sup> cells/well for further culture. The cells were used for experiments when the confluence was about 80%. Quantitative polymerase chain

reaction (qPCR) assay was carried out to detect the expression level of miR-129-2 in HepG2 and L-02 cells.

### Cell Transfection

HepG2 cells in serum-free DMEM were inoculated in a 6-well plate, with cell density adjusted to 3×10<sup>5</sup> cells/well. MiR-129-2 mimic/negative control or Lipofectamine™2000 was diluted with serum-free DMEM at 1:50, and let stand at 25°C for 5 min. Then, the mixture of transfection plasmid and Lipofectamine™2000 was added to the 6-well plate with cultured cells and cultured in the 5% CO<sub>2</sub> incubator at 37°C for 2 d. Blank control group, negative control group, and over-expression group were set.

### QRT-PCR Assay

Tissue samples or cultured cells were collected, lysed in TRIzol (Thermo Fisher Scientific, Waltham, MA, USA) for 5 min on ice and incubated with 700 µL of chloroform. The mixture was shaken and centrifuged at 10,000 g, 4°C for 10 min. Next, the supernatant was aspirated, and an equal volume of isopropanol was added. After centrifugation at 10,000 g, 4°C for 10 min, the precipitate was washed with 1 mL of freshly prepared 75% ethanol, shaken repeatedly, and centrifuged at 10,000 g at 4°C for 5 min. The precipitant was air dried and dissolved in 0 µL of diethyl pyrocarbonate (DEPC) water (Beyotime, Shanghai, China). The purity and concentration of RNA samples were detected. QRT-PCR system was prepared in strict accordance with the instructions of a reverse transcription kit (Invitrogen, Carlsbad, CA, USA), and the RNA was reversely transcribed into complementary deoxyribose nucleic acid (cDNA) under the adjusted conditions of 37°C for 15 min and 85°C for 5 s. QRT-PCR was performed at 95°C pre-denaturation for 30 s, 95°C denaturation for 5 s, and 60°C annealing for 30 s, for a total of 35 cycles. The

Table I. Primer sequences

| Gene      |           | Sequences                 |
|-----------|-----------|---------------------------|
| MiR-129-2 | Sense     | GGGGGATCGCGGACGGTCTGGAGAA |
|           | Antisense | CAGCGCGTTCCATCGCGGCTCAG   |
| GAPDH     | Sense     | GAGTCAACGGATTTGGTGGT      |
|           | Antisense | TTGATTTTGAGGGGATCTC       |
| U6        | Sense     | CTCGCTTCGGCAGCAC          |
|           | Antisense | AACGCTTCACGAATTTGCGT      |

amplification was carried out using a qRT-PCR instrument, and the primers were synthesized by Invitrogen (Carlsbad, CA, USA), with glyceraldehyde-3-phosphate dehydrogenase (GAPDH) as an internal reference. The sequences were shown in Table I. The expression level of miR-129-2 was calculated by  $2^{-\Delta\Delta Ct}$ .

#### **Determination of Cell Proliferation Via Methyl Thiazolyl Tetrazolium (MTT) Assay**

Transfected cells were seeded in a 96-well plate at  $3 \times 10^4$  cells/well. They were cultured in serum-free DMEM for 24 h. On the other day, 0.5 mg/mL MTT was added and cultured for 4 h. After that, the medium was discarded, and 150  $\mu$ L of dimethyl sulfoxide (DMSO) was added. Lastly, a microplate reader was utilized for recording the absorbance value, and the proliferation of cells in each group was calculated.

#### **Detection of Apoptosis of Cells Through Flow Cytometry**

Transfected cells were seeded in a 6-well plate at  $5 \times 10^5$  cells/well in serum-free DMEM for 24 h. Cells were collected in Eppendorf (EP; Hamburg, Germany) tubes and washed with phosphate-buffered saline (PBS) for three times. Flow apoptosis detection kit (BD, Franklin Lakes, NJ, USA) was used for determining cell apoptosis. 20  $\mu$ L of PE antibody, 20  $\mu$ L of 7-AAD antibody, and 1 mL of diluent were added to each tube, mixed, and reacted in a dark place for 15 min. The apoptosis level was measured by flow cytometry. All samples should be detected within 1 h.

#### **Wound Healing Assay**

After successful transfection, the cells were collected and cultured till the logarithmic growth phase. Then, the cells in the set blank control group, negative control group, and overexpression group were inoculated into a 6-well plate at  $5 \times 10^5$  cells/well and cultured with serum-containing DMEM in the 5% CO<sub>2</sub> incubator at 37°C for 24 h. After that, a marking pen was employed to draw horizontal lines on the back of the 6-well plate, and a 10  $\mu$ L pipette was used to make scratches along the horizontal lines. Next, the cells falling off were cleared by PBS washing, and the remaining attached cells attached were incubated with serum-free DMEM in the 5% CO<sub>2</sub> incubator at 37°C for 24 h. Wound closure in the 6-well plate was photographed using a microscope at 0 h and 24 h after scratching.

#### **Western Blotting**

Radioimmunoprecipitation assay (RIPA) lysis buffer (Beyotime, Shanghai, China) at a ratio of 1 mg: 1 mL, with 1% protease inhibitor and 1% phosphatase inhibitor was added in cells. After centrifugation at 12,000 g, 4°C for 10 min, the total protein was collected. The concentration of protein was determined using a bicinchoninic acid (BCA) protein assay kit (Pierce, Rockford, IL, USA). An equal concentration of protein samples was prepared by adding loading buffer, and boiled at 95°C for 15 min. After that, sodium dodecyl sulphate-polyacrylamide gel electrophoresis (SDS-PAGE) were prepared, and the proteins were subjected to electrophoresis under constant pressure, transferred to a polyvinylidene difluoride (PVDF) membrane (IPVH00010, Millipore, Billerica, MA, USA). Membranes were blocked in 5% skim milk for 2 h, cut into small pieces according to the indicated sizes and incubated with primary antibodies against Sox4, matrix metalloproteinase-2 (MMP-2), glycogen synthase kinase-3 $\beta$  (GSK3 $\beta$ ), phosphorylated GSK3 $\beta$  (p-GSK3 $\beta$ ), and GAPDH (CST, Danvers, MA, USA, diluted at 1:1,000) in a refrigerator at 4°C overnight. Then, the bands were washed with phosphate-buffered saline with Tween<sup>®</sup>-20 (PBST), incubated with horseradish peroxidase (HRP)-conjugated secondary antibodies (Shanghai Yinhai Sheng Biotechnology Co., Ltd., Shanghai, China, diluted at 1:5,000) at room temperature for 1 h, and washed using PBST. Thereafter, enhanced chemiluminescence (ECL) solution (Millipore, Billerica, MA, USA) was added and followed by band exposure. Lastly, the bands were scanned, and the expression level of relevant proteins was calculated.

#### **Modeling**

A total of 36 nude mice aged 6 weeks old were purchased from the Experimental Animal Center of Southern Medical University and they were housed in a Specific Pathogen Free (SPF) environment. Transfected liver cancer cells in the logarithmic growth phase were collected from overexpression (high expression of miR-129-2) group, negative control group, and blank control group, and prepared into single cell suspension with a cell density of  $5 \times 10^7$  cells/mL. Next, 0.2 mL of the cell suspension was injected subcutaneously into each nude mouse. These mice were divided into overexpression group (n=12), negative control group (n=12), and blank control group

(n=12). The growth of tumors in each group was observed. At 30 d after modeling, nude mice were sacrificed for collecting tumors. The volume and weight of tumors were measured. This investigation was approved by the Animal Ethics Committee of Southern Medical University Animal Center.

### Statistical Analysis

The data in this study were expressed as mean  $\pm$  standard deviation and analyzed by Statistical Product and Service Solutions (SPSS) 22.0 software (IBM, Armonk, NY, USA). The Chi-square test was used for enumeration data. Analysis of variance (ANOVA) was employed for comparison among groups.  $p < 0.05$  suggested that the difference was statistically significant.

## Results

### Expression Level of MiR-129-2 in Liver Cancer Tissues and Cell Lines

QRT-PCR was employed to measure the expression level of miR-129-2 in liver cancer tissues and HepG2 cells. The results showed that the expression level of miR-129-2 was clearly lower in liver cancer tissues than that in adjacent tissues ( $p < 0.01$ ), and it was significantly lower in HepG2 cell line than that in normal liver L-02 cell ( $p < 0.01$ ; Figure 1).

### Constructed Liver Cancer Cell Line with Overexpressed MiR-129-2

Liver cancer cell line HepG2 with overexpressed miR-129-2 was constructed by transfection of miR-129-2 mimic, and then the expression level of miR-129-2 was determined through qPCR. It was found that the expression level of miR-129-2 was markedly higher in overexpression group than that in negative control group ( $p < 0.01$ ; Figure 2), indicating the effective transfection efficacy.

### Effects of MiR-129-2 on Proliferation of Liver Cancer Cells

MTT assay was conducted to detect the influence of miR-129-2 on the proliferation of liver cancer cells. It is revealed that the proliferation ability was evidently weakened in overexpression group compared with that in negative control group ( $p < 0.01$ ; Figure 3).

### Influences of MiR-129-2 on Apoptosis of Liver Cancer Cells

The influence of miR-129-2 on the apoptosis of cells in each group was determined by flow cytometry. The results demonstrated that the apoptosis level was higher in overexpression group than that in negative control group ( $p < 0.01$ ; Figure 4).

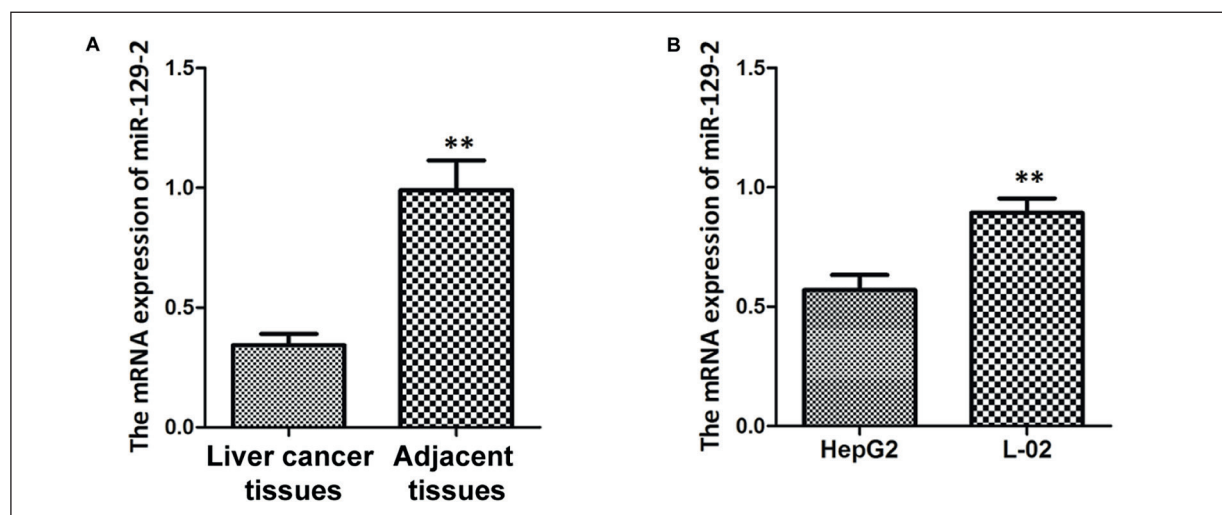


**Figure 1.** Expression level of miR-129-2 detected *via* qPCR. (A) Expression level of miR-129-2 in liver cancer tissues and adjacent tissues, and (B) Expression level of miR-129-2 in liver cancer cell lines and normal liver cells. The expression level of miR-129-2 evidently declines in liver cancer tissues compared with that in adjacent tissues (\*\* $p < 0.01$  vs. liver cancer tissues), and it is significantly reduced in HepG2 cells compared with that in L-02 cells (\*\* $p < 0.01$  vs. HepG2 cells).



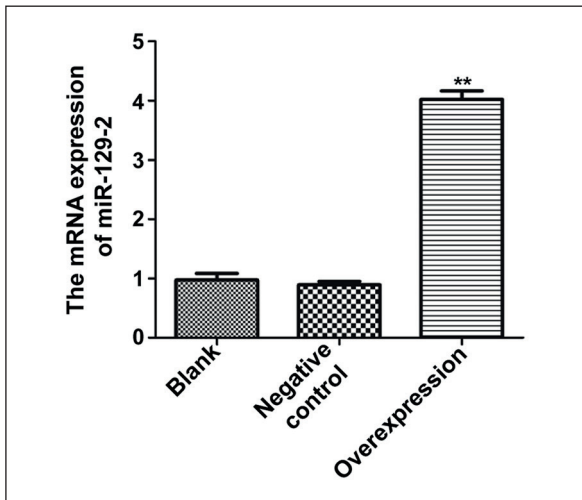


**Figure 2.** Constructed liver cancer cell line with overexpressed miR-129-2. Compared with that in blank and negative control groups, the expression level of miR-129-2 is overtly elevated in overexpression group (\*\* $p < 0.01$  vs. negative control group).

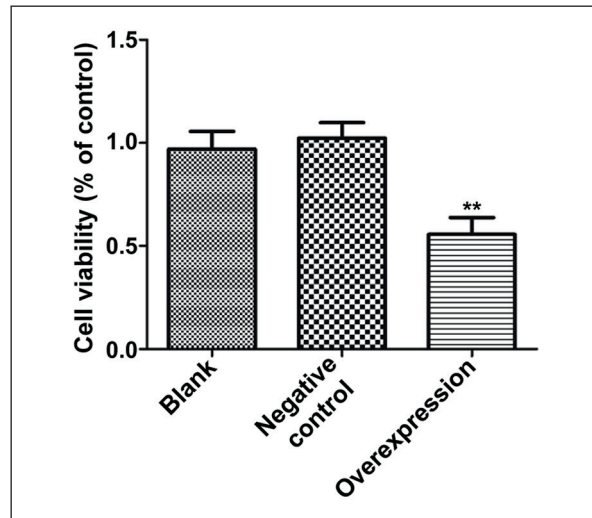


**Figure 3.** Proliferation level of liver cancer cells detected via MTT. The proliferation ability of cells is overtly lower in overexpression group than that in blank and negative control groups (\*\* $p < 0.01$  vs. negative control group).

**Impacts of MiR-129-2 on Migration of Liver Cancer Cells**

Wound healing assay was performed to examine the impact of miR-129-2 on the migration of liver cancer cells. Distance between the scratch-

es in each group was detected at 0 h and 24 h, respectively. It was discovered that the distance between the scratches was remarkably longer in overexpression group than that in negative control group ( $p < 0.01$ ; Figure 5).

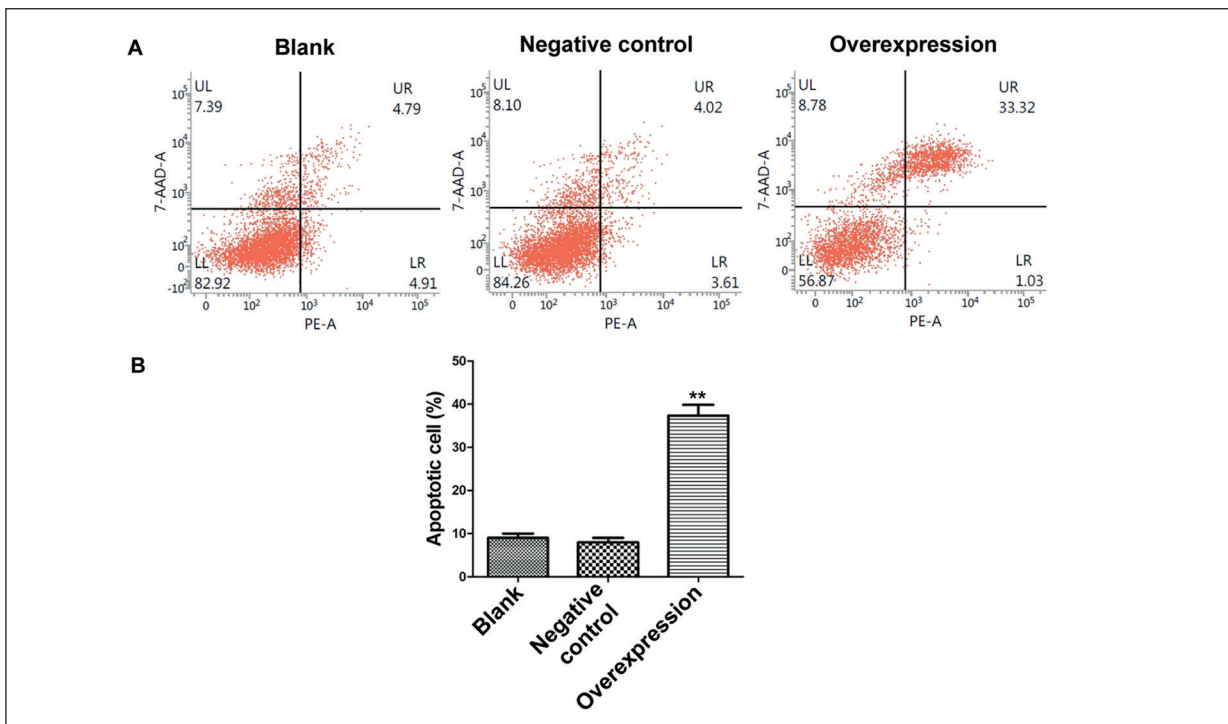


**Figure 4.** Apoptosis level of liver cancer cells detected via flow cytometry. The apoptosis level is overtly higher in overexpression group than that in blank and negative control groups, (\*\* $p < 0.01$  vs. negative control group).

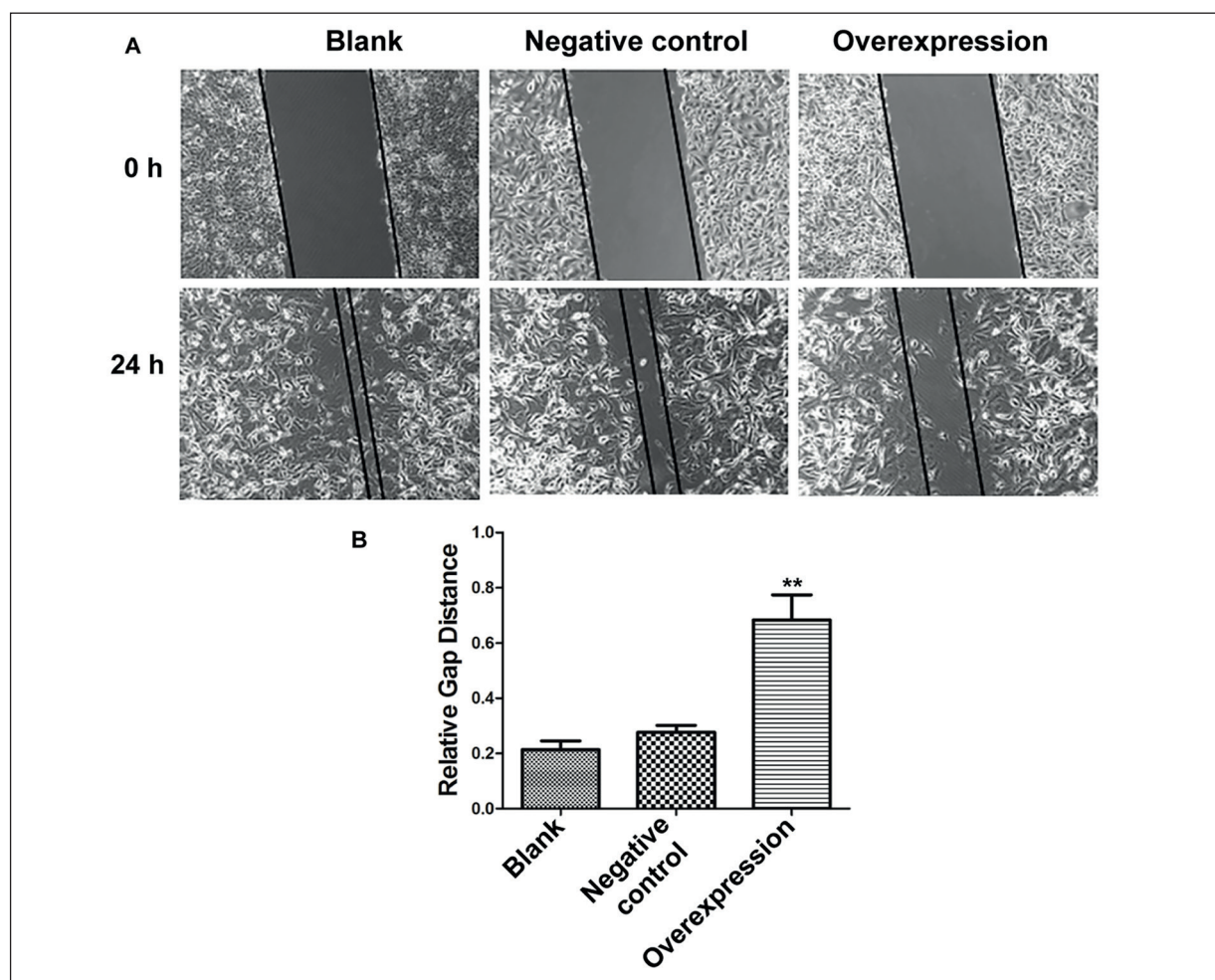


**Figure 5.** Migration capacity of liver cancer cells detected *via* wound healing assay (magnification: 40×). (A) Cell micrograph, and (B) Statistical chart. The distance between the scratches is markedly longer in overexpression group than that in blank and negative control groups (\*\* $p < 0.01$  vs. negative control group).

### Effects of MiR-129-2 on Wnt Signaling Pathway-Related Proteins

The expression levels of Wnt signaling pathway-related proteins in liver cancer cells were determined by Western blotting. The results uncovered that the expression levels of Sox4 and MMP-2 were significantly lower in overexpression group than those in negative control group ( $p < 0.01$ ), while the expression level of p-GSK3 $\beta$  was overtly higher in overexpression group than that in negative control group ( $p < 0.01$ ; Figure 6).

### Tumor Volume And Weight in Nude Mice Bearing Liver Cancer

At 30 d after the establishment of *in vivo* xenograft tumor model in nude mice, the tumor in each mouse was collected. The volume and

weight of tumors in nude mice were clearly smaller in overexpressing group than those in negative control group ( $p < 0.01$ ; Figure 7).

## Discussion

As a common malignant tumor, liver cancer has a high mortality rate, which severely affects the life quality of affected patients<sup>9</sup>. Currently, gene detection and gene intervention therapy are important prevention and treatment methods for malignant tumors<sup>10</sup>. In recent years, clinical potentials of miRNAs in the prevention and treatment of cancers have attracted increasing attention. Ishida et al<sup>11</sup> discovered that the abnormal expression level of miR-129-2 is closely related to the development and progression of esophagus

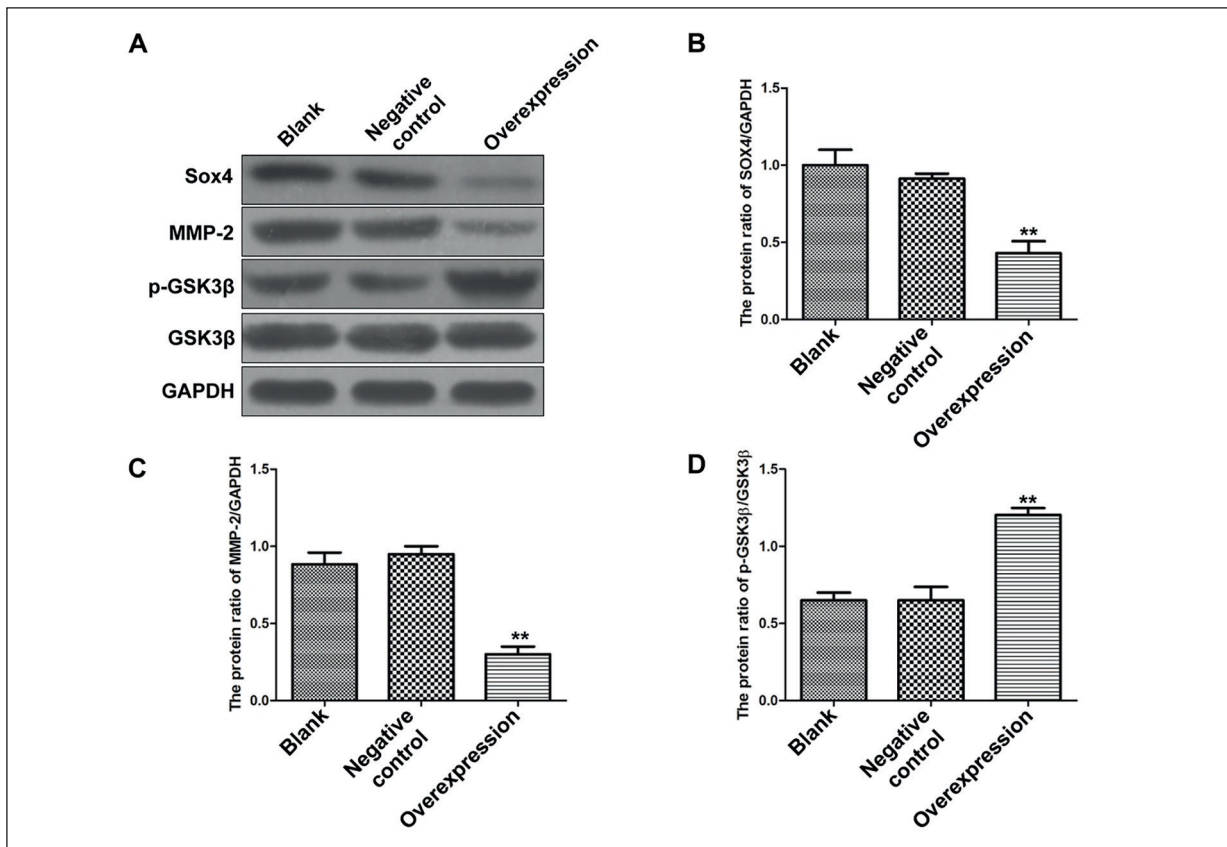


**Figure 6.** Expression level of Wnt signaling pathway-related proteins in liver cancer cells determined by Western blotting. (A) Protein band diagram, (B) Statistical chart of Sox4 protein expression, (C) Statistical chart of MMP-2 protein expression, and (D) Statistical chart of p-GSK3 $\beta$  protein expression. Overexpression group has evidently raised expression levels of Sox4 and MMP-2 and an overtly decreased expression level of p-GSK3 $\beta$  in cells in comparison with blank and negative control groups (\*\* $p < 0.01$  vs. negative control group).

cancer. In this study, the expression level of miR-129-2 in cancer tissues and adjacent tissues of 20 patients with liver cancer was analyzed. The results revealed that the expression of miR-129-2 was significantly lower in liver cancer tissues than that in adjacent tissues. In addition, further analysis of miR-129-2 expression level in liver cancer cells HepG2 displayed that the expression level of miR-129-2 was also significantly lower in liver cancer cells than that in normal liver cells.

MiR-129-2 is transcribed from small non-coding RNA precursor molecules, which is involved in regulating the expressions of various genes and proteins. Meanwhile, miR-129-2 is significantly downregulated in many tumors, including bladder cancer, stomach cancer, and endometrial carcinoma, leading to the poor overall survival and life quality of patients<sup>12-14</sup>. In this study, overexpression of miR-129-2 overtly reduced the protein expressions of Sox4 and MMP-2 in liver cancer

cells. The invasion and migration abilities of tumor cells are the key events for the metastasis of tumor cells. Tumor cells metastasize to other tissues and organs through invasion and migration<sup>15</sup>. The MMP family proteins can effectively degrade the extracellular matrix. MMP-2, a non-glycated IV collagenase, is able to enter the forefront of the matrix and degrade the cell matrix. Highly expressed MMP-2 in cancer tissues can promote the migration of tumor cells, while suppressing MMP-2 is capable of significantly weakening the invasion and migration ability of tumor cells<sup>16</sup>. Zhang et al<sup>17</sup> demonstrated that the interference in MMP-2 expression in osteosarcoma cells significantly inhibits the invasion and migration of osteosarcoma cells. Ge et al<sup>18</sup> found that inhibiting Sox4 expression in lung cancer cells reduces the expression of the downstream gene MMP-2, which is consistent with our findings. In this study, it was also uncovered that

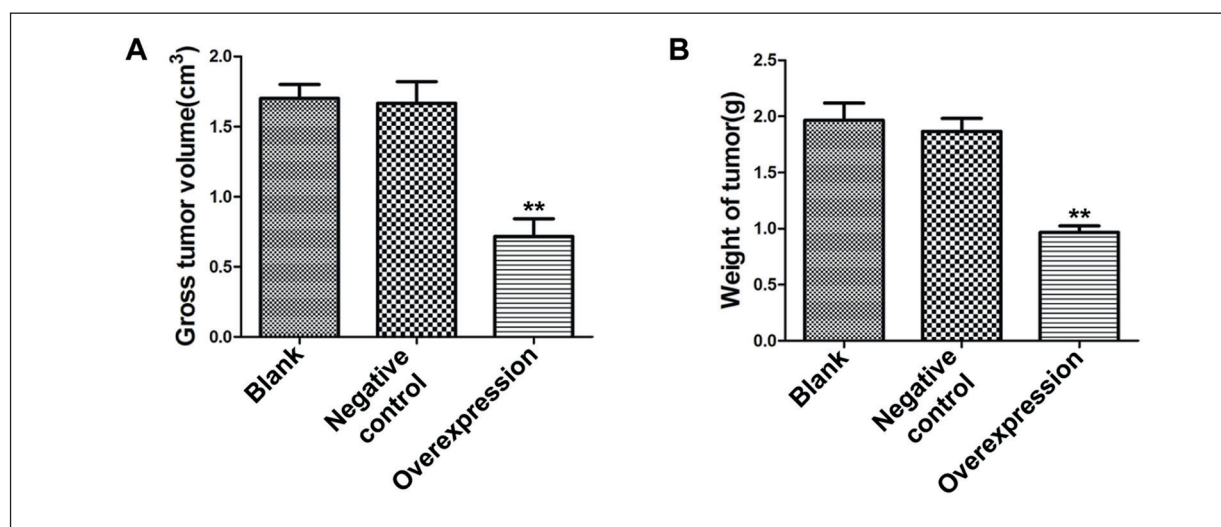


**Figure 7.** Volume and weight of tumors in nude mice bearing liver cancer. (A) Statistical chart of tumor volume, and (B) Statistical chart of mass. The volume and weight of tumors in nude mice are remarkably smaller in overexpression group than those in blank and negative control groups (\*\* $p < 0.01$  vs. negative control group).

overexpressing miR-129-2 markedly weakened the proliferation capacity of liver cancer cells HepG2 and elevated the apoptosis level. Besides, the *in vivo* xenograft tumor model in nude mice bearing liver cancer identically suggested the role of miR-129-2 in regulating the growth of tumors. It is believed that overexpression of miR-129-2 is able to repress the proliferation and migration, and facilitate the apoptosis of liver cancer cells.

Chi et al<sup>19</sup> found that activating the Wnt signaling pathway in tumor cells can markedly elevate the proliferation and invasion abilities of colorectal cancer cells. We discovered that overexpressing miR-129-2 in liver cancer cells inhibits the intracellular expression of Sox4, thereby raising the phosphorylation level of GSK-3 $\beta$  in liver cancer cells. GSK-3 $\beta$ , a typical multiplex protein kinase, can be phosphorylated at different sites to play different physiological roles. The increased phosphorylation level of GSK-3 $\beta$  lowers the activity of GSK-3 $\beta$ , inhibits the Wnt signaling pathway, and alleviates the proliferation, invasion, and migration capacities of tumor cells<sup>20</sup>.

## Conclusions

We found through *in vivo* and *in vitro* experiments that the expression level of miR-129-2 overtly declines in liver cancer tissues and cells. Overexpression of miR-129-2 represses the ex-

pressions of Sox4 and MMP-2, and inactivates the Wnt signaling pathway, thus weakening the proliferation and migration abilities of liver cancer cells and promoting the apoptosis. Our findings provide new ideas for the diagnosis and treatment of liver cancer.

## Conflict of Interest

The Authors declare that they have no conflict of interests.

## References

- 1) FARHAT F, TARABAIH M, KANJ A, AOUN M, KATTAN J, ASSI T, AWADA A. Palbociclib safety and efficacy beyond Ribociclib-induced liver toxicity in metastatic hormone-receptors positive breast cancer patient. *Anticancer Drugs* 2020; 31: 85-98.
- 2) WANG JB, BAI ZF, XIAO XH. Is aristolochic acid the major cause of liver cancer in China and Asia? *Hepatology* 2019 Oct 14. doi: 10.1002/hep.30993. [Epub ahead of print].
- 3) TSILIMIGRAS DI, BAGANTE F, MORIS D, MERATH K, PAREDES AZ, SAHARA K, RATTI F, MARQUES HP, SOUBRANE O, LAM V, POULTSIDES GA, POPESCU I, ALEXANDRESCU S, MARTEL G, WORKNEH A, GUGLIELMI A, HUGH T, ALDRIGHETTI L, ENDO I, PAWLIK TM. Defining the chance of cure after resection for hepatocellular carcinoma within and beyond the Barcelona Clinic Liver Cancer Guidelines: a multi-institutional analysis of 1,010 patients. *Surgery* 2019; 166: 967-974.
- 4) CAI J, ZHENG J, XIE Y, KIRIH MA, TAO L, LIANG X. Laparoscopic repeat hepatectomy for treating recurrent



- liver cancer. *J Minim Access Surg* 2019 Oct 11. doi: 10.4103/jmas.JMAS\_187\_19. [Epub ahead of print].
- 5) CHEN J, ZHANG Y, CAI H, YANG Y, FEI DY. Comparison of the effects of postoperative prophylactic transcatheter arterial chemoembolization (TACE) and transhepatic arterial infusion (TAI) after hepatectomy for primary liver cancer. *J BUON* 2018; 23: 629-634.
  - 6) DUROUX-RICHARD I, ROBIN M, PEILLEX C, APPARAILLY F. MicroRNAs: fine tuners of monocyte heterogeneity. *Front Immunol* 2019; 10: 2145.
  - 7) GODBOLE M, CHANDRANI P, GARDI N, DHAMNE H, PATEL K, YADAV N, GUPTA S, BADWE R, DUTT A. miR-129-2 mediates down-regulation of progesterone receptor in response to progesterone in breast cancer cells. *Cancer Biol Ther* 2017; 18: 801-805.
  - 8) KLANGJORHOR J, CHAIYAWAT P, TEEYAKASEM P, SIRIKAEW N, PHANPHAISARN A, SETTAKORN J, LIRDPRAPAMONGKOL K, YAMA S, SVASTI J, PRUKSAKORN D. Mycophenolic acid is a drug with the potential to be repurposed for suppressing tumor growth and metastasis in osteosarcoma treatment. *Int J Cancer* 2019 Oct 14 doi: 10.1002/ijc.32735. [Epub ahead of print]
  - 9) LIN H, FAN T, SUI J, WANG G, CHEN J, ZHUO S, ZHANG H. Recent advances in multiphoton microscopy combined with nanomaterials in the field of disease evolution and clinical applications to liver cancer. *Nanoscale* 2019; 11: 19619-19635.
  - 10) ASHRAFIZADEH M, AHMADI Z, MOHAMMADINEJAD R, FARKHONDEH T, SAMARGHANDIAN S. MicroRNAs mediate the anti-tumor and protective effects of ginsenosides. *Nutr Cancer* 2019: 1-12.
  - 11) ISHIDA T, MAKINO T, YAMASAKI M, TANAKA K, MIYAZAKI Y, TAKAHASHI T, KUROKAWA Y, MOTOORI M, KIMURA Y, NAKAJIMA K, MORI M, DOKI Y. Impact of measurement of skeletal muscle mass on clinical outcomes in patients with esophageal cancer undergoing esophagectomy after neoadjuvant chemotherapy. *Surgery* 2019; 166: 1041-1047.
  - 12) MITASH N, TIWARI S, AGNIHOTRI S, MANDHANI A. Bladder cancer: microRNAs as biomolecules for prognostication and surveillance. *Indian J Urol* 2017; 33: 127-133.
  - 13) KAUR S, LOTSARI JE, AL-SOHAILY S, WARUSAVITARNE J, KOHONEN-CORISH MR, PELTOMAKI P. Identification of subgroup-specific miRNA patterns by epigenetic profiling of sporadic and Lynch syndrome-associated colorectal and endometrial carcinoma. *Clin Epigenetics* 2015; 7: 20.
  - 14) CAO HY, XIAO CH, LU HJ, YU HZ, HONG H, GUO CY, YUAN JF. MiR-129 reduces CDDP resistance in gastric cancer cells by inhibiting MAPK3. *Eur Rev Med Pharmacol Sci* 2019; 23: 6478-6485.
  - 15) YU Y, ABUDULA M, LI C, CHEN Z, ZHANG Y, CHEN Y. Icotinib-resistant HCC827 cells produce exosomes with mRNA MET oncogenes and mediate the migration and invasion of NSCLC. *Respir Res* 2019; 20: 217.
  - 16) YANG J, ZHANG J, XING J, SHI Z, HAN H, LI Q. Inhibition of proliferation and migration of tumor cells through phenylboronic acid-functionalized poly-amidoamine-mediated delivery of a therapeutic DNAzyme Dz13. *Int J Nanomedicine* 2019; 14: 6371-6385.
  - 17) ZHANG X, QU P, ZHAO H, ZHAO T, CAO N. COX2 promotes epithelialmesenchymal transition and migration in osteosarcoma MG63 cells via PI3K/AKT/NFkappaB signaling. *Mol Med Rep* 2019; 20: 3811-3819.
  - 18) GE T, WU HC, ZHOU YY, SHEN SM, ZHU LG, YOU GX. MiR-296-3p may affect the proliferation and migration of non-small cell lung cancer cells via regulating RABL3. *Eur Rev Med Pharmacol Sci* 2019; 23: 5823-5830.
  - 19) CHI J, ZHANG H, HU J, SONG Y, LI J, WANG L, WANG Z. AGR3 promotes the stemness of colorectal cancer via modulating Wnt/beta-catenin signalling. *Cell Signal* 2020; 65: 109419.
  - 20) WANG J, YANG J, CHENG X, YIN F, ZHAO Y, ZHU Y, YAN Z, KHODAEI F, OMMATI MM, MANTHARI RK, WANG J. Influence of calcium supplementation against fluoride-mediated osteoblast impairment in vitro: involvement of the canonical Wnt/beta-catenin signaling pathway. *J Agric Food Chem* 2019; 67: 10285-10295.